http://doi.org/10.35784/iapgos.8115 received: 17.07.2025 | revised: 28.08.2025 | accepted: 14.09.2025 | available online: 30.09.2025

METHODS AND MEANS OF LASER LAYER JONES MATRIX MAPPING OF POLYCRYSTALLINE FILMS OF BIOLOGICAL FLUIDS

Olexander Ushenko[1,2], Iryna Soltys[2], Olexander Dubolazov[2], Sergii Pavlov[3], Vasyl Garasym[2], Alona Kolomiiets[3], Bakhyt Yeraliyeva[4]

[1]Taizhou Institute of Zhejiang University, Taizhou, China, [2]Chernivtsi National University, Chernivtsi, Ukraine, [3] Vinnytsia National Technical University, Vinnitsa, Ukraine, [4]M. Kh. Dulaty Taraz Regional University, Taraz, Kazakhstan

Abstract. *The results of the theoretical substantiation and experimental validation of a novel laser polarization-interference method for Jones matrix mapping with digital phase layer-by-layer scanning of the object field of polycrystalline bile films are presented. Statistical analysis of the layer-by-layer maps of the real and imaginary components of the Jones matrix images has revealed a set of diagnostic markers – skewness and kurtosis – sensitive to variations in the linear and circular birefringence of the polycrystalline structure within the supramolecular networks of dehydrated bile films.*

Keywords: Jones matrix, polarization, interferometry, linear and circular birefringence, central statistical moments, bile

METODY I ŚRODKI LASEROWEGO MAPOWANIA MACIERZY JONESA WARSTW POLIKRYSTALICZNYCH PŁYNÓW BIOLOGICZNYCH

Streszczenie. *Przedstawiono wyniki teoretycznego uzasadnienia oraz eksperymentalnej weryfikacji nowej laserowej metody polaryzacyjno-interferencyjnego mapowania macierzy Jonesa z cyfrowym, warstwowym skanowaniem fazowym pola obiektu polikrystalicznych rozmazów żółci. Analiza statystyczna warstwowych map rzeczywistych i urojonych składowych obrazów macierzy Jonesa ujawniła zestaw markerów diagnostycznych – skośność i kurtozę – wrażliwych na zmiany dwójłomności liniowej i kołowej w strukturze polikrystalicznej sieci supramolekularnych odwodnionych rozmazów żółci.*

Słowa kluczowe: macierz Jonesa, polaryzacja, interferometria, liniowa i kołowa dwójłomność, centralne momenty statystyczne, żółć

Introduction

In recent years, modern non-destructive and non-invasive optical diagnostic methods for biological tissue samples have been widely and effectively applied across various fields of medicine [5, 9, 19]. Among the broad spectrum of optical methods, one of the most effective has emerged – laser polarimetric diagnostics of the polycrystalline structure of biological layers [2, 6, 11]. The methodological generalization and further development of laser polarimetry have resulted in multiparametric Mueller-matrix polarimetry methods and systems that deliver comprehensive information on pathological and necrotic alterations in the optically anisotropic components of biological tissues [7, 16, 17]. A new frontier in expanding the functional capabilities and improving the sensitivity of differential diagnostics of various pathological and necrotic conditions in Mueller-matrix polarimetry has been the development of innovative 3D scanning techniques for biological sample volumes [1, 4, 10].

It should be noted that the vast majority of laser polarimetry methods and systems are primarily aimed at defining criteria and practical applications in the differential diagnosis and monitoring of pathological and necrotic changes in human organ tissues [8, 12, 14]. However, the detection criteria for the polycrystalline structure of biological fluid films remain largely unexplored and are of significant current interest [3, 13, 20]. These objects carry valuable information about the overall state of the body, are easily accessible, and do not require a traumatic biopsy procedure. From a fundamental perspective, studying such weakly scattering and volumetrically inhomogeneous films within laser polarimetry requires the application of the Jones-matrix formalism [8, 15].

This study is devoted to the theoretical substantiation and experimental validation of a novel multifunctional laser polarization-interference approach for Jones matrix mapping of polycrystalline bile films, incorporating digital phase scanning of their supramolecular networks [7, 16, 20].

The applied component of the study focuses on selecting statistical parameters most sensitive to structural changes in bile films, represented by the spatial distributions of the complex Jones matrix elements [17, 18].

1. Brief theory of the method

Each partial layer of the polycrystalline blood film is considered a phase plate with a certain phase retardation of linear birefringence (*LB*). Circular birefringence (*CB*) causes the rotation of the polarization plane, which is characterized by an azimuthal angle.

$$\phi(z) = \gamma z \tag{1}$$

where z is the propagation direction or the geometric path in the phase layer, and γ is a constant.

Let δ be the phase shift of linear birefringence *LB* in the absence of polarization plane rotation or circular birefringence *CB*.

$$\delta = \frac{2\pi}{\lambda}\Delta n l \tag{2}$$

where l – the total thickness of the polycrystalline film.

The total thickness of the polycrystalline film

$$\phi_0 = \phi(l) = \gamma l \tag{3}$$

We assume that:

- the phase retardation in the volume of each partial layer is N times smaller than δ (relation (2));
- the partial layer with index m is oriented at an azimuthal angle of $m\zeta$ (relation (1)), where $\zeta = \frac{\gamma_0}{N}\varphi$.

$$\{J\} = \prod_{m=1}^{N}\{R(m\zeta)\}\{J_0\}\{R(-m\zeta)\} \tag{4}$$

here, $\{R(m\zeta)\}$ i $\{R(-m\zeta)\}$ are rotation matrices.

For further analysis of expression (4), we used well-known relations between rotation matrices

$$\{R(\zeta_1)\}\{R(\zeta_2)\} = \{R(\zeta_1 + \zeta_2)\} \tag{5}$$

Taking into account (5), expression (4) can be rewritten as:

$$\{J\} = \{R(\phi_0)\}[\{J_0\}\{R(-\zeta)\}]^N \tag{6}$$

where

$$\{J_0\} = \begin{Vmatrix} exp\left(-i\frac{\delta}{2N}\right) & 0 \\ 0 & exp\left(i\frac{\delta}{2N}\right) \end{Vmatrix} \tag{7}$$

Thus,

$$\{J\} = \{R(\phi_0)\} = \begin{Vmatrix} cos\,\zeta\, exp\left(-i\frac{\delta}{2N}\right) & -sin\,\zeta\, exp\left(-i\frac{\delta}{2N}\right) \\ sin\,\zeta\, exp\left(i\frac{\delta}{2N}\right) & cos\,\zeta\, exp\left(i\frac{\delta}{2N}\right) \end{Vmatrix}^2 \tag{8}$$

Since matrix (8) is unimodular, we applied Chebyshev's identity

$$\begin{Vmatrix} F_{11} & F_{12} \\ F_{21} & F_{22} \end{Vmatrix}^{m} = \begin{Vmatrix} F_{11}Q_{m-1} - Q_{m-2} & F_{12}Q_{m-1} \\ F_{21}Q_{m-1} & F_{22}Q_{m-1} - Q_{m-2} \end{Vmatrix} \quad (9)$$

where

$$Q_m = \frac{sin[(N+1)TH]}{sin\,TH} \quad (10)$$

$$cos[TH] = \frac{F_{11}+F_{22}}{2} \quad (11)$$

Taking into account (9)–(11), the equations (8) take the following form:

$$J_{11} = (J_{22})^* = cos\left(\frac{\zeta_0}{N}\right) exp\left[-i\left(\frac{\delta}{2N}\right)\frac{sin(N\theta)}{sin\,\theta} - \frac{sin((N-1)\theta)}{sin\,\theta}\right] \quad (12)$$

$$J_{12} = -(J_{21})^* = -sin\left(\frac{\zeta_0}{N}\right) exp\left[-i\left(\frac{\delta}{2N}\right)\frac{sin(N\theta)}{sin\,\theta}\right] \quad (13)$$

$$cos\,\theta = cos\left(\frac{\zeta_0}{N}\right) cos\left(\frac{\delta}{2N}\right) \quad (14)$$

The relations (12) – (14) can be simplified by performing the limit transition as $N \to \infty$. For this purpose, we expanded all "cosines" into their Taylor series

$$\theta^2 = \left(\frac{\zeta}{N}\right)^2 + \left(\frac{\delta}{2N}\right)^2 \quad (15)$$

and introduced new notations

$$U^2 = N^2\theta^2 = \zeta^2 + \left(\frac{\delta}{2}\right)^2 \quad (16)$$

As a result, the Jones matrix $\{J\}$ of an optically thin phase-anisotropic ("*LB+CB*") layer of the biological fluid facies takes the following analytical form:

$$\{J\} = \begin{Vmatrix} cos\,U - i\frac{\delta\,sin\,U}{2U} & -\zeta\frac{sin\,U}{U} \\ \zeta\frac{sin\,U}{U} & cos\,U + i\frac{\delta\,sin\,U}{2U} \end{Vmatrix} \quad (17)$$

Expression (17) provides an exact analytical representation of the set of elements of the Jones matrix for an optically anisotropic layer with linear (δ) and circular (ζ) birefringence.

2. Jones matrix mapping method for bile films

The method of polarization interferometry for mapping the distribution of complex Jones matrix elements includes the following experimental steps and algorithmic actions:

1. Two collinear states of linear polarization are sequentially formed in the "illuminating" (Ir) and "reference" (Re) parallel laser beams – $Ir(0^0) - Re(\,0^0)$ and $Ir(90^0) - Re(\,90^0)$.
2. For each formed state of linear polarization, two partial interference patterns are recorded by rotating the transmission plane of the polarizer-analyzer 13 at angles $\Omega = 0^0;\ \ \Omega = 90^0$.
3. For each experimentally recorded partial interference distribution of the laser object field of the polycrystalline phase of the biological fluid sample, a digital two-dimensional Fourier transform is applied.

$$\begin{cases} j_{11} = \frac{1}{A\times B}\sum_{a=0}^{A-1}\sum_{b=0}^{B-1} E_x^0(E_x^0)^*(a,b)\, e^{\left[-i2\pi\left(\frac{a\times v}{A}+\frac{b\times v}{B}\right)\right]} \\ j_{12} = \frac{1}{A\times B}\sum_{a=0}^{A-1}\sum_{b=0}^{B-1} E_y^0\left(E_y^0\right)^*(a,b)\, e^{\left[-i2\pi\left(\frac{a\times v}{A}+\frac{b\times v}{B}\right)\right]} \\ j_{21} = \frac{1}{A\times B}\sum_{a=0}^{A-1}\sum_{b=0}^{B-1} E_x^{90}(E_x^{90})^*(a,b)\, e^{\left[-i2\pi\left(\frac{a\times v}{A}+\frac{b\times v}{B}\right)\right]} \\ j_{22} = \frac{1}{A\times B}\sum_{a=0}^{A-1}\sum_{b=0}^{B-1} E_y^{90}\left(E_y^{90}\right)^*(a,b)\, e^{\left[-i2\pi\left(\frac{a\times v}{A}+\frac{b\times v}{B}\right)\right]} \end{cases} \quad (18)$$

where $E_{x,y}^{0,90}$ are the orthogonal components of the complex amplitude for different orientations of the transmission plane of the polarizer-analyzer $\Omega = 0^0;\ \ \Omega = 90^0$; $*$ – denotes the complex conjugation operation; (v, v) – represent the spatial frequencies; and (a = 1120, b = 960) indicate the number of pixels of the digital CCD camera.

4. The results of the two-dimensional digital Fourier transform of the intensity distributions of polarization-filtered partial interference patterns are used for the algorithmic reconstruction of the complex amplitude field formed by the sample of the polycrystalline optically anisotropic phase of the biological fluid, following the algorithm below.

$$\begin{cases} E_{0^0} \to |E_x^0(\Omega = 0^0)| \\ E_{90^0} \to |E_x^{90}(\Omega = 90^0)|\, exp\left(i(\varphi_x^{90} - \varphi_x^0)\right) \end{cases} \quad (19)$$

$$\begin{cases} E_{0^0} \to \left|E_y^0(\Omega = 0^0)\right| \\ E_{90^0} \to \left|E_y^{90}(\Omega = 90^0)\right|\, exp\left(i\left(\varphi_y^{90} - \varphi_y^0\right)\right) \end{cases} \quad (20)$$

3. Analysis and discussion of experimental results

The outcomes of the experimental layer-by-layer polarization-interference Jones matrix mapping [3, 7, 17–19] of dehydrated bile films are illustrated in a series of fragments shown in Figs. 1, 2.

The analysis of the obtained data revealed:

- An individual coordinate structure of the Jones matrix distributions $Re(j_{ik}(m\times n))$ of the complex dendritic-spherulitic polycrystalline networks is observed in Fig. 1, fragments (1), (2), and (5), (6).
- Asymmetric distributions of histograms $G(Re(j_{ik}))$ of the matrix elements $Re(j_{11;12;21;22})$ of the dehydrated polycrystalline bile film are shown in Fig. 1, fragments (3), (4), and (7), (8).
- A distinct phase transformation of the topographic and statistical structure of the Jones matrix images $Re(j_{ik}(m\times n))$ with respect to the phase shift θ_k is shown in Fig. 2, fragments (3), (4), and (7), (8).

The results of the transformation of Jones matrix images $Re\left(j_{ik}(m\times n)\right)$ of the bile film are presented in table 1.

Table 1. Statistical moments of the 1st to 4th orders characterizing the Jones matrix images of the bile film

$Re\{J_{ik}\}$				
Z_i	$Re\{J_{11}\}$	$Re\{J_{12}\}$	$Re\{J_{21}\}$	$Re\{J_{22}\}$
Z_1	0.52±0.027	0.47±0.025	0.41±0.022	0.45±0.024
Z_2	0.34±0.018	0.33±0.017	0.26±0.014	0.28±0.016
Z_3	0.11±0.006	0.22±0.012	0.18±0.011	0.23±0.13
Z_4	0.19±0.011	0.34±0.018	0.23±0.013	0.35±0.018
$\varphi = \pi/4$				
Z_i	$Re\{J_{11}\}$	$Re\{J_{12}\}$	$Re\{J_{21}\}$	$Re\{J_{22}\}$
Z_1	0.46±0.025	0.41±0.022	0.32±0.017	0.38±0.021
Z_2	0.29±0.017	0.22±0.012	0.17±0.09	0.21±0.011
Z_3	0.35±0.019	0.24±0.013	0.19±0.011	0.41±0.022
Z_4	0.47±0.025	0.36±0.019	0.25±0.013	0.58±0.031

It was established that:

- There is a distinct statistical distribution, different from the normal ($Z_{3;4} = 0$), for the set of Jones matrix images $Re(j_{ik}(m\times n))$ of the polycrystalline networks of bile.
- Opposite trends in the change of the mean ($Z_{i=1}$), variance ($Z_{i=2}$), skewness ($Z_{i=3}$), and kurtosis ($Z_{i=4}$), which characterize the transformation of Jones matrix images $Re(j_{ik}(m\times n))$ in different phase planes ($\varphi_k(m\times n)$) of the polycrystalline bile film, are observed as $\begin{pmatrix} Z_{1;2}\downarrow \\ Z_{3,4}\uparrow \end{pmatrix}$.
- The values of the mean and variance $Z_{i=1;2}(Re(j_{ik}(m\times n)))$ slightly decrease with an increase in the phase scanning parameter $\varphi_k \uparrow$ (within the range of 30% to 50%).
- The values of the higher-order statistical moments $Z_{i=3;4}(Re(j_{ik}(m\times n)))$, which characterize the skewness and kurtosis of the distributions of the real (Re) components of the matrix elements $Re(j_{11;12;21;22})$, significantly increase (up to 6 times) as the phase scanning parameter $\theta_k \uparrow$ increases.

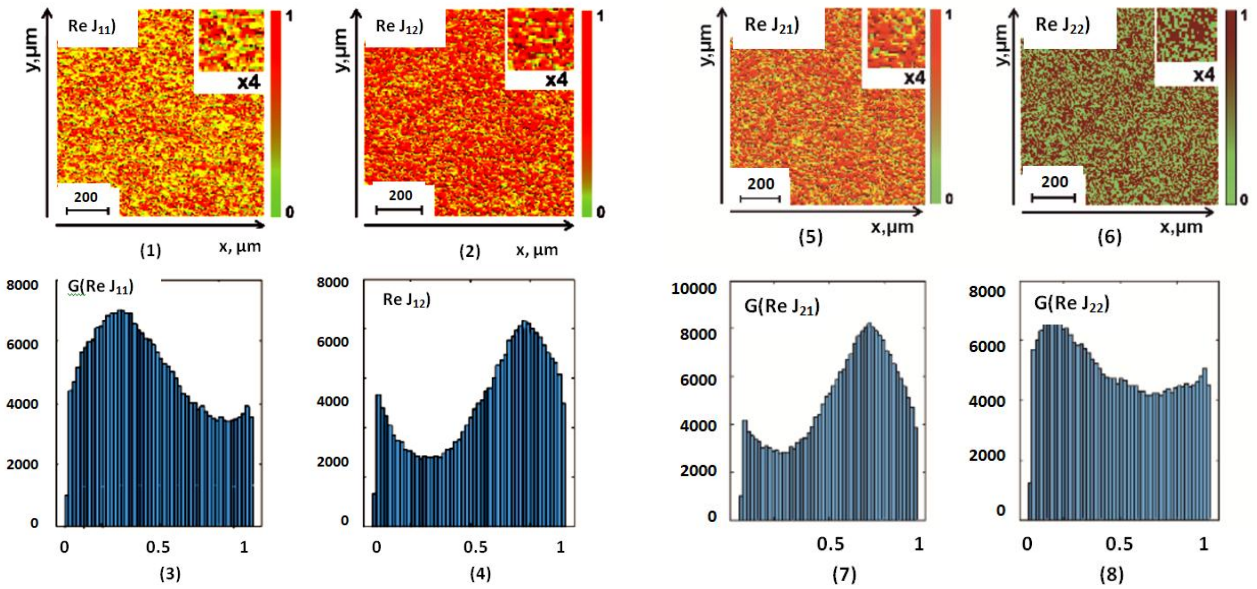

Fig. 1. Integral coordinate and statistical structure of the real parts of the Jones matrix the sisograms $J_{ik}(m \times n)$ for the complex dendritic-spherulitic polycrystalline network of the dehydrated bile film

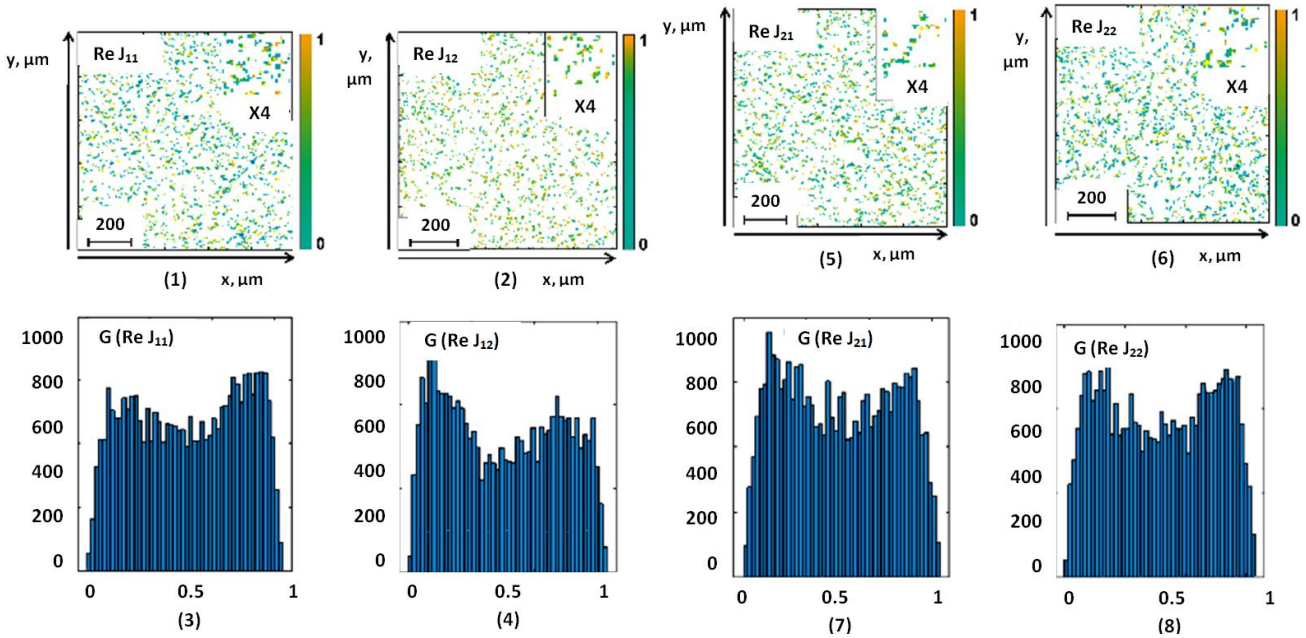

Fig. 2. Layer-by-layer ($\varphi = \pi/4$) coordinate and statistical structure of the real parts of Jones matrix images of the dehydrated bile film

From a physical standpoint, the results obtained can be attributed to specific features of the structural organization of complex dendritic-spherulitic polycrystalline networks in dehydrated bile films. In addition to the optically isotropic component (an optically homogeneous micellar solution containing small amounts of cylindrical epithelial cells, leukocytes, leukocytoids, and mucus), bile also includes an optically anisotropic component – a liquid-crystalline phase composed of three types of liquid crystals: needle-shaped fatty acid crystals (LFA), cholesterol monohydrate crystals (CHM), and calcium bilirubinate (CB).

At the dehydration stage, an optically crystalline solid phase is formed through dendritic and disclination crystallization mechanisms. The dendritic pathway converts the liquid-crystalline optically anisotropic fraction into aggregates of solid, needle-shaped, optically uniaxial birefringent crystals. In contrast, the disclination mechanism of the liquid-crystalline phase gives rise to a solid crystalline fraction composed of rectangular and rhomboidal CHM crystals. Additionally, during concretion formation, pronounced calcium bilirubinate (CB) deposits and microspherulites of calcium carbonate are observed.

Thus, a complex dendritic-spherulitic polycrystalline structure of the dehydrated bile film is formed. Therefore, along with variations in the directions of the optical axes γ of the needle-like crystals of the dendritic network of the dehydrated bile film, the values of the real (*Re*) components of the matrix elements $Re(j_{11;22})$ are influenced by the optically anisotropic properties of the calcium carbonate microspherolites and the rectangular, rhomboidal crystals of CHM.

As a result, the values of the 1st- and 2nd-order statistical moments, reflecting the mean and variance of the distributions, were obtained of $Re(j_{11;22})$, are slightly smaller compared to the similar statistical parameters that characterize the mean and variance of the coordinate distributions of the real components of the Jones matrix elements of the polycrystalline bile films (table 1).

In addition, the real components of the Jones matrix elements $Re(j_{12;21})$, which characterize the mutual transformations of polarization states due to the optical activity of the biological crystals, are practically comparable to the values of the real components of the collection of elements $Re(j_{11;22})$.

This fact indicates a significant influence of the optical activity of chiral molecular domains in the dehydrated bile film on the manifestation of structural anisotropy in the networks of needle-like crystals.

Finally, as the phase scanning shift $\varphi_k \downarrow$ decreases, a more optically thin volume of the dehydrated bile film is distinguished. As a result, two effects arise:

- the distribution of the optical axis orientations of the needle-like crystals transforms from a nearly uniform distribution ($0 \le \gamma \le 2\pi$) into an asymmetric one ($\gamma_{min} \le \gamma \le \gamma_{max}$).
- the concentration of spherulitic optically active molecular domains decreases.

Accordingly, the statistics of the Jones matrix thesisograms $Re(j_{11;12;21;22}(m \times n))$ change as $\begin{pmatrix} Z_{1;2} \downarrow; \\ Z_{3;4} \uparrow \end{pmatrix}$.

Notably, the most sensitive statistical parameters (table 1) to such transformations in the polycrystalline dendritic-spherulitic structure of the dehydrated bile film are the 3rd and 4th order statistical moments, which describe the skewness and kurtosis of the coordinate distributions of the real components of all partial elements $Re(j_{11;12;21;22}(m \times n))$ of the Jones matrix.

4. Conclusions

1. The study presents and analyzes the experimental verification of the proposed polarization-interference mapping method with digital reconstruction of complex amplitude distributions in phase-inhomogeneous object fields, as well as the algorithmic calculation of coordinate distributions of Jones matrix elements in a series of phase sections of dehydrated bile films.
2. The typical scenarios of statistical transformations in the structure of Jones matrix images across successive layers of the polycrystalline component of dehydrated bile films have been identified and physically interpreted.
3. A set of the most informative diagnostic indicators for detecting changes in the orientation-phase organization of polycrystalline networks in dehydrated biological fluid films has been determined – namely, the 3rd- and 4th-order statistical moments, reflecting the skewness and kurtosis of the coordinate distributions of Jones matrix elements.
4. The maximum variation ranges of statistical indicators as the phase scanning step increases have been established, with values reaching a 5- to 8-fold change.

Acknowledgments

The authors gratefully acknowledge the support of the National Research Foundation of Ukraine under Project 2023.03/0174.

Disclosures

No conflicts of interest are declared by the authors.

Ethics approval and consent to participate

This research was carried out in accordance with the principles of the Declaration of Helsinki, adhering to the International Conference on Harmonization – Good Clinical Practice guidelines and applicable local regulations. Ethical approval was granted by the Ethics Committee of Bukovinian State Medical University (Chernivtsi, Ukraine) under protocol No. 7 dated May 16, 2024.

References

[1] Angelsky O. V., et al.: Handbook of Photonics for Biomedical Science. CRC press, 2010, 22–67.
[2] Burkovets D. N., et al.: Stokes polarimetry of biotissues. Fourth International Conference on Correlation Optics 3904, 1999, 527–533.
[3] Chen W., et al.: Extended eigenvalue calibration method for Mueller matrix polarimetry with four photoelastic modulators. Opt. Lett. 50(3), 2025, 840–843.
[4] Garazdyuk M. S., et al.: Polarization-phase images of liquor polycrystalline films in determining time of death. Applied optics 55 (12), 2016, B67–B71
[5] Ghosh N.: Tissue polarimetry: concepts, challenges, applications, and outlook. J. Biomed. Opt. 1, 2011, 110801.
[6] Jacques S. L.: Polarized light imaging of biological tissues. Boas D., Pitris C., Ramanujam N. (eds.): Handbook of Biomedical Optics 2. CRC Press, 2011, 649–669.
[7] Jiao W., et al.: Analysis and optimization of the pixel saturation effect on backscattering Mueller matrix polarimetry. Opt. Lett. 50, 2025, 5069–5072.
[8] Jóźwicki R., et al.: Automatic polarimetric system for early medical diagnosis by biotissue testing. Optica Applicata 32 (4), 2002, 603–612.
[9] Kukharchuk V. V., et al.: Information Conversion in Measuring Channels with Optoelectronic Sensors, Sensors 22(1), 2022, 271 [https://doi.org/10.3390/s22010271].
[10] Layden D., Ghosh N., Vitkin I. A.: Quantitative polarimetry for tissue characterization and diagnosis. Wang R. K., Tuchin V. V. (eds.): Advanced Biophotonics: Tissue Optical Sectioning. CRC Press, 2013, 73–108.
[11] Liu T., et al.: Comparative study of the imaging contrasts of Mueller matrix derived parameters between transmission and backscattering polarimetry. Biomed. Opt. Express 9(9), 2018, 4413–4428.
[12] Oberemok Ye. A., et al.: Influence of imperfections of polarization elements on measurement errors in three probing polarizations method. Proc. SPIE 6164, 2006, 61640B.
[13] Pishak V., et al.: Study of polarization structure of biospeckle fields in crosslinked tissues of human organism: 1. Vector structure of skin biospeckles. Proc. SPIE 3317, 1997, 418–424.
[14] Romanyuk A. N., et al.: Fast ray casting of function-based surfaces. Przeglad Elektrotechniczny 93(5), 2017, 83–86.
[15] Vasilevskyi O. et al: Methods for Constructing High-precision Potentiometric Measuring Instruments of Ion Activity. IEEE 41st International Conference on Electronics and Nanotechnology – ELNANO, 2022, 247–252.
[16] Vitkin A., Ghosh N., de Martino A.: Tissue Polarimetry. Andrews D. L. (ed.): Photonics: Scientific Foundations, Technology and Applications. John Wiley & Sons, Ltd. 2015, 239–321.
[17] Yermolenko S., et al.: Spectropolarimetry of cancer change of biotissues. Proc. SPIE 7388, 2009, 73881D [https://doi.org/10.1117/12.853585].
[18] Zabolotna N., et al.: Diagnostic efficiency of Mueller-matrix polarization reconstruction system of the phase structure of liver tissue. Proc. SPIE 9816, 2015, 98161E [https://doi.org/10. 1117/12.2229018].
[19] Zabolotna N. I., et al.: ROC analysis of informativeness of mapping of the ellipticity distributions of blood plasma films laser images polarization in the evaluation of pathological changes in the breast. Proc. SPIE 11456, 2020, 114560I.
[20] Zhang Z., et al.: Analysis and optimization of aberration induced by oblique incidence for in-vivo tissue polarimetry. Opt. Lett. 48(23), 2023, 6136–6139.

Prof. Olexander Ushenko
e-mail: o.ushenko@chnu.edu.ua

He is a Doctor of Physics and Mathematics, Head of the Department of Optics and Publishing and Printing at Yuriy Fedkovych Chernivtsi National University, Chernivtsi, Ukraine.

https://orcid.org/0000-0001-7015-7423

Ph.D. Iryna Soltys
e-mail: i.soltys@chnu.edu.ua

Iryna Soltys is a Ph.D. in Physics and Mathematics. Associate professor at the Department of Optics and Publishing and Printing at Yuriy Fedkovych Chernivtsi National University, Chernivtsi, Ukraine.

https://orcid.org/0000-0003-2156-7404

Prof. Olexander Dubolazov
e-mail: a.dubolazov@chnu.edu.ua

Oleksandr Dubolazov is a Doctor of Physics and Mathematics. Professor at the Department of Optics and Publishing and Printing at Yuriy Fedkovych Chernivtsi National University Chernivtsi, Ukraine.

https://orcid.org/0000-0003-1051-2811

Prof. Sergii Pavlov
e-mail: psv@vntu.edu.ua

Academician of International Applied Radioelectronic Science Academy. Professor of Biomedical Engineering and Optic-Electronic Systems Department, Vinnytsia National Technical University.

https://orcid.org/0000-0002-0051-5560

Mr. Vasyl Garasym
e-mail: v.harasym@chnu.edu.ua

Vasyl Garasym is a Ph.D. student in Optics, Laser Physics at the Department of Optics Publishing and Printing at Yuriy Fedkovych Chernivtsi National University Chernivtsi, Ukraine.

https://orcid.org/0009-0009-4284-2736

D.Sc. Alona Kolomiiets
e-mail: alona.kolomiets.vnt@gmail.com

Doctor of Pedagogical Sciences, associate professor, professor of Department of Higher Mathematics, Vinnytsia National Technical University.
Research interests: professional pedagogy, the fundamentalization of the mathematical training of future bachelors of technical specialties, mathematical modeling, methods of statistical analysis of experimental data.

https://orcid.org/0000-0002-7665-6247

Ph.D. Bakhyt Yeraliyeva
e-mail: yeraliyevabakhyt81@gmail.com

Senior lecturer of the Information Systems Department, Faculty of Information Technology, M. Kh. Dulaty Taraz Regional University, Taraz, Kazakhstan.
Research interests: fiber optic technologies, information systems, internet of things and blockchain technologies.

https://orcid.org/0000-0002-8680-7694